



ARL-TN-1027 • SEP 2020



# A Python Script for Calculating Magnetization in Alloys

by Efraín Hernández-Rivera, Heather A Murdoch, Anit K Giri,  
and Matthew C Guziewski

Approved for public release; distribution is unlimited.

## **NOTICES**

### **Disclaimers**

The findings in this report are not to be construed as an official Department of the Army position unless so designated by other authorized documents.

Citation of manufacturer's or trade names does not constitute an official endorsement or approval of the use thereof.

Destroy this report when it is no longer needed. Do not return it to the originator.



# **A Python Script for Calculating Magnetization in Alloys**

**by Efraín Hernández-Rivera, Heather A Murdoch, Anit K Giri,  
and Matthew C Guziewski**

*Weapons and Materials Research Directorate, CCDC Army Research Laboratory*

REPORT DOCUMENTATION PAGE			Form Approved OMB No. 0704-0188		
<p>Public reporting burden for this collection of information is estimated to average 1 hour per response, including the time for reviewing instructions, searching existing data sources, gathering and maintaining the data needed, and completing and reviewing the collection information. Send comments regarding this burden estimate or any other aspect of this collection of information, including suggestions for reducing the burden, to Department of Defense, Washington Headquarters Services, Directorate for Information Operations and Reports (0704-0188), 1215 Jefferson Davis Highway, Suite 1204, Arlington, VA 22202-4302. Respondents should be aware that notwithstanding any other provision of law, no person shall be subject to any penalty for failing to comply with a collection of information if it does not display a currently valid OMB control number.</p> <p><b>PLEASE DO NOT RETURN YOUR FORM TO THE ABOVE ADDRESS.</b></p>					
1. REPORT DATE (DD-MM-YYYY) September 2020		2. REPORT TYPE Technical Note		3. DATES COVERED (From - To) October 2017-July 2019	
4. TITLE AND SUBTITLE A Python Script for Calculating Magnetization in Alloys			5a. CONTRACT NUMBER		
			5b. GRANT NUMBER		
			5c. PROGRAM ELEMENT NUMBER		
6. AUTHOR(S) Efraín Hernández-Rivera, Heather A Murdoch, Anit K Giri, and Matthew C Guziewski			5d. PROJECT NUMBER		
			5e. TASK NUMBER		
			5f. WORK UNIT NUMBER		
7. PERFORMING ORGANIZATION NAME(S) AND ADDRESS(ES) US Army Combat Capabilities Development Command Army Research Laboratory ATTN: FCDD-RLW-MB Aberdeen Proving Ground, MD 21005-5066			8. PERFORMING ORGANIZATION REPORT NUMBER ARL-TN-1027		
9. SPONSORING/MONITORING AGENCY NAME(S) AND ADDRESS(ES)			10. SPONSOR/MONITOR'S ACRONYM(S)		
			11. SPONSOR/MONITOR'S REPORT NUMBER(S)		
12. DISTRIBUTION/AVAILABILITY STATEMENT Approved for public release; distribution is unlimited.					
13. SUPPLEMENTARY NOTES corresponding author's email: <efrain.hernandez18.civ@mail.mil>; ORCIDs: Efraín Hernández-Rivera 0000-0002-7855-1027, Heather A Murdoch 0000-0001-7710-0577, Anit K Giri 0000-0003-0085-9846, Matthew C Guziewski 0000-0002-5761-720X					
14. ABSTRACT Magnetization of a material is an important property that influences how it interacts with magnetic fields. Therefore, it is important to accurately calculate and/or predict magnetization of a wide range of material alloys. The Weiss mean field theory model and Kuz'min equation of state are explored in the technical note. Their formulations are briefly described, followed by a few examples applied to iron-based alloys. The Python module for calculating the magnetization is included as an appendix.					
15. SUBJECT TERMS magnetization, Weiss mean field theory, Kuz'min equation of state					
16. SECURITY CLASSIFICATION OF:			17. LIMITATION OF ABSTRACT UU	18. NUMBER OF PAGES 29	19a. NAME OF RESPONSIBLE PERSON Efraín Hernández-Rivera
a. REPORT Unclassified	b. ABSTRACT Unclassified	c. THIS PAGE Unclassified			19b. TELEPHONE NUMBER (Include area code) 410-306-4961

## Contents

---

<b>List of Figures</b>	<b>iv</b>
<b>List of Tables</b>	<b>v</b>
<b>1. Introduction</b>	<b>1</b>
<b>2. Model Formulations</b>	<b>1</b>
2.1 Weiss Mean Field Theory	2
2.2 Magnetization for Alloys	3
2.3 Kuz'min Equation of State	4
<b>3. Analysis of Models</b>	<b>6</b>
3.1 WMFT Model	6
3.2 KEoS Model	8
3.3 Model Comparison	11
<b>4. Conclusions</b>	<b>12</b>
<b>5. References</b>	<b>13</b>
<b>Appendix A. Weiss mean field theory (WMFT) and Kuz'min Equation of State (KEoS) Python Script</b>	<b>15</b>
<b>List of Symbols, Abbreviations, and Acronyms</b>	<b>21</b>
<b>Distribution List</b>	<b>22</b>

## List of Figures

---

- Fig. 1 Fe magnetization as calculated by WMFT, showing a) curves for  $j = 0.5$  (solid) and  $j = 1$  (dashed) and b) the percent difference between the different  $j$  values. This shows that the error decreases as the applied field  $H$  increases. ....7
- Fig. 2 Instability observed for WMFT when calculating the magnetization for the Fe-10Ni alloy .....8
- Fig. 3 WMFT prediction of magnetization as a function of alloy composition for the a) FeCo and b) FeNi systems .....9
- Fig. 4 Performance of KEoS in predicting magnetization of Fe. a) Comparing the Kuz'min (solid) and WMFT (dashed) models, which show that there's a limit to Kuz'min as the applied field goes up. b) reduced temperature limit at the saturation magnetization ( $\tau|_{\sigma=1}$ ) as a function of applied field..... 10
- Fig. 5 KEoS prediction of magnetization as a function of alloy composition for the a) FeCo and b) FeNi systems ..... 11
- Fig. 6 Comparison between WMFT and KEoS calculated magnetization for elemental a) Fe, b) Ni, and c) Co. It is clear that Kuz'min better approximates the experimental data. .... 12

## List of Tables

---

---

Table 1	Material parameters for WMFT, which describe the influence of alloying on the Curie temperature and magnetic moment in Fe (after Ishikawa <sup>11</sup> )	7
Table 2	Values of the parameters used for KEoS .....	10

## 1. Introduction

---

One of the more important properties of magnetic materials is their magnetization, which influences how a material behaves when exposed to a magnetic field. For instance, it has been observed that processing under a magnetic field influences a phase's alignment and spacing<sup>1,2</sup> and the formation of metastable carbide precipitates.<sup>3,4</sup> This is a result of the magnetic field influencing the thermodynamics of the system, wherein competing kinetic and thermodynamic mechanisms are at play. The strength that a magnetic field will have on a material's behavior can be captured through the description of the thermodynamic component as a function of magnetization:

$$\Delta G_{mag}^{ext} = -\mu_0 \int_0^H M(H, T, x) dH \quad (1)$$

where  $\mu_0$  is the permeability of vacuum,  $H$  is the externally applied magnetic field,  $T$  is the processing temperature, and  $x$  is the alloy composition.

Several models (e.g., Weiss mean field theory [WMFT]) have been used to simulate and/or predict an alloy's magnetization. To fully explore some of these models, Murdoch et al. [5] performed a robust analysis and comparison of some of these models. This technical note provides some further observations on the WMFT and Kuz'min's equation of state (KEoS) models, and a more detailed description of how these models were implemented. Furthermore, the `python` class used to calculate the magnetization based on these models is included in the Appendix.

## 2. Model Formulations

---

Multiple models have been developed to predict and/or fit the magnetization of a given material. Two of these are the WMFT and Landau models, which have been successfully used to describe magnetization in a variety of materials. Here, we focus on these two models, which were recently extended to model magnetization in alloys.<sup>5</sup>



## 2.1 Weiss Mean Field Theory

---

WMFT denotes the magnetization of an ensemble of  $N$  atoms, each with a magnetic moment  $m$  when subjected to an externally applied magnetic field  $H$ :

$$M = mNB_j(\alpha) = M_0B_j(\alpha) \quad (2)$$

where  $M_0 = mN$  is the saturation magnetization and  $B_j$  is the Brillouin function

$$B_j(\alpha) = \frac{2j+1}{2j} \coth\left(\frac{2j+1}{2j}\alpha\right) - \frac{1}{2j} \coth\left(\frac{1}{2j}\alpha\right) \quad (3)$$

and the quantum number  $j$  is a positive integer or half-integer. The  $\alpha$ -parameter is defined as the ratio of the Zeeman energy of the magnetic moment and the thermal energy

$$\alpha = \frac{m(H + wM)}{k_B T} \quad (4)$$

where  $w$  is the molecular field constant and  $k_B$  is the Boltzmann constant. The term  $wM$  gives the internal magnetization field. The Curie temperature, at which magnetization goes to zero in the absence of an applied external field, can be defined as

$$T_C = \frac{(j+1)wm^2N}{3jk_B} \quad (5)$$

Since the molecular field constant can have a complex dependence on the material's electronic structure, causing it to vary widely between species, it is convenient to remove it by using Eq. 5,

$$w = \frac{3jk_B T_C}{(j+1)m^2N}, \quad (6)$$

which, by combining with Eqs. 2 and 4, we can express  $\alpha$  as

$$\alpha = \frac{mH}{k_B T} + \frac{3jk_B T_C}{(j+1)m^2N} \frac{mM}{k_B T} = \frac{mH}{k_B T} + \frac{3jB_j(\alpha) T_C}{j+1} \frac{1}{T}. \quad (7)$$

Rearranging Eq. 7, we can derive the ‘‘transcendental equation’’

$$B_j(\alpha) - \frac{j+1}{3j} \frac{T}{T_C} \alpha + \frac{j+1}{3j} \frac{mH}{k_B T_C} = 0, \quad (8)$$

which must be solved numerically. This nonlinear equation was solved using the `nsolve` function of Python's `sympy` module.

## 2.2 Magnetization for Alloys

---

To properly account for alloying, the existing treatment varies the Curie temperature and magnetic moment linearly as a function of alloy composition. A description of how to extend WMFT to alloys, adopted from Guo and Enomoto,<sup>6,7</sup> is presented next. For example, an iron (Fe)-based material (Fe-M) has a Curie temperature given by

$$T_C^a = T_C^{Fe}(1 + a \cdot x^M) \quad (9)$$

and a magnetic moment by

$$m = m^{Fe}(1 + b \cdot x^M), \quad (10)$$

where  $a$  and  $b$  are material parameters. These material parameters can be obtained experimentally measuring how the Curie temperature and magnetic moment changes as a function of composition

$$a = \frac{100}{T_C^{Fe}} \frac{dT_C}{dx^M} \quad (11a)$$

$$b = \frac{1}{m^{Fe}} \frac{dm}{dx^M}. \quad (11b)$$

The magnetization of the binary alloy is calculated by

$$M = mNB_j(\alpha + \Delta\alpha) \quad (12)$$

where  $\Delta\alpha = Ax$  is the alloying-induced change in  $\alpha$ . Performing a first-order Taylor expansion and using Eq. 10, we get

$$\begin{aligned} M &= m^{Fe} N \cdot [1 + b \cdot x^M] \cdot [B_j(\alpha) + x^M AB'_j(\alpha)] \\ M &= m^{Fe} N \cdot [B_j(\alpha) + x^M AB'_j(\alpha) + b \cdot x^M B_j(\alpha) + b \cdot x^{M+1} B'_j(\alpha)]. \end{aligned} \quad (13)$$

Finally, only keeping terms that depend linearly with  $x^M$ , we get

$$M = m^{Fe} N [B_j(\alpha) + \{A \cdot B'_j(\alpha) + b \cdot B_j(\alpha)\} \cdot x^M] \quad (14)$$

Examining Eq. 14, it can be observed that we still need to determine the  $A$  param-

eter. In order to derive a function for  $A$ , we can extend Eq. 8 to its alloyed form:

$$B_j(\alpha + \Delta\alpha) - \frac{j+1}{3j} \frac{(\alpha + \Delta\alpha)T}{T_C^{Fe}(1 + ax^M)} + \frac{j+1}{3jk_B} \frac{m^{Fe}(1 + bx^M)H}{T_C^{Fe}(1 + ax^M)} = 0. \quad (15)$$

Keeping in mind that  $B_j(\alpha + \Delta\alpha) = B_j(\alpha) + \Delta\alpha B'_j(\alpha)$ , performing some expansion with respect to  $x^M$  and grouping by order, we get

$$0^{\text{th}} : B_j(\alpha) - \frac{j+1}{3j} \frac{T}{T_C} \alpha + \frac{(j+1)mH}{3jk_B T_C} \quad (16a)$$

$$1^{\text{st}} : AB'_j(\alpha) + aB_j(\alpha) - \frac{j+1}{3j} \frac{T}{T_C^{Fe}} A + \frac{(j+1)m^{Fe}Hb}{3jk_B T_C^{Fe}} \quad (16b)$$

$$2^{\text{nd}} : aAB'_j(\alpha). \quad (16c)$$

Then, recognizing that  $B_j(\alpha)$  corresponds to the pure alloy and combining Eq. 8 (for Fe) and the first-order terms of Eq. 16, we get

$$AB'_j(\alpha) - \frac{j+1}{3j} \frac{T}{T_C^{Fe}} (A - a\alpha) + \frac{(j+1)}{3j} \frac{m^{Fe}H}{k_B T_C^{Fe}} (b - a) = 0, \quad (17)$$

and finally, we can solve for  $A$ :

$$A = \frac{k_B T a \alpha + m^{Fe} H (b - a)}{k_B T - 3j T_C^{Fe} B'_j(\alpha) / (j + 1)}. \quad (18)$$

It should be noted that once the  $\alpha$  values for a given elemental system subjected to an applied field  $H$  are obtained, these values can be used to calculate the magnetization of the alloy based on the elemental system. Hence, we only need to calculate the  $\alpha$  values as a function of  $H$  and  $T$  once and then reuse these for alloyed systems.

### 2.3 Kuz'min Equation of State

---

Based on Landau's theory for ferromagnets,<sup>8</sup> Kuz'min developed an approximate equation of state (EoS).<sup>9</sup> This EoS applies to ferromagnets at  $T \lesssim T_C$  undergoing a second-order phase transition.

Following the ferromagnet-specific version of Landau theory, as stated by Ginzburg,<sup>10</sup> a thermodynamic potential can be written as an expansion of magnetization:

$$\Phi(M, H, T) = \Phi_0 + \frac{1}{2}AM^2 + \frac{1}{4}BM^4 + \frac{1}{6}CM^6 + \dots - HM \quad (19)$$

where the coefficients  $\Phi_0, A, B, C, \dots$  may depend on external thermodynamic parameters (e.g., temperature), but not on the applied field  $H$ . Under thermodynamic equilibrium, we get

$$\frac{\partial \Phi}{\partial M} = AM + BM^3 + CM^5 + \dots - H = 0, \quad (20)$$

which is an implicit form of the magnetic EoS, giving a relation between  $M, H$ , and  $T$ . Given the reduced magnetization ( $\sigma = M/M_0$ ) and temperature ( $\tau = T/T_C$ ), the magnetic EoS can be rewritten as

$$H = a\sigma + b\sigma^3 + c\sigma^5 + \dots \quad (21)$$

where  $a, b$ , and  $c$  are functions of the reduced temperature. Kuz'min postulated that the magnetic EoS can be expressed as Eq. 21 when: 1) it has been truncated to the  $\sigma^5$  term, 2) coefficients  $b$  and  $c$  are independent of  $\tau$ , and 3) coefficient  $a$  dependence on  $\tau$  fulfills Bloch's 3/2 power law at low temperatures:

$$a(\tau) = a_0 \frac{\tau^3 - 1}{1 + p\tau^{3/2}} \quad (22)$$

where  $a_0, p$  and  $\kappa = b/a_0$  are material parameters. Then, with the normalization condition

$$\sigma(T = 0, H = 0) = 1 \quad \rightarrow \quad M = M_0 \quad (23)$$

we get

$$H = a_0\sigma \left[ \frac{\tau^3}{1 + p + \tau^{3/2}} + \kappa\sigma^2 + (1 - \kappa)\sigma^4 \right] \quad (24)$$

where  $a_0, p$  and  $\kappa = b/a_0$  are material parameters. An alternative to solving this problem, the EoS can be solved for  $\tau$ :

$$\tau = \left( \sqrt{1 - 2u + p^2u^2} - pu \right)^{2/3} \quad (25)$$

where

$$u = \frac{1}{2} \left[ \kappa\sigma^2 + (1 - \kappa)\sigma^4 - \frac{H}{a_0\sigma} \right]. \quad (26)$$

It should be noted that either equation could be used to fit to experimental data, where Eq. 24 can be used to fit experimental magnetization curves ( $\sigma$  vs.  $H$ , with fixed  $\tau$ ), while Eq. 26 can be used to fit temperature dependences of magnetization

at a fixed magnetic field ( $\sigma$  vs.  $\tau$ , with fixed  $H$ ).

### 3. Analysis of Models

---

This section explores how these models perform at predicting the magnetization of different metals. We consider both pure systems, and the influence of alloying through the WMFT model.

#### 3.1 WMFT Model

---

WMFT has been used to calculate magnetization for pure Fe across a range of applied fields, as shown in Fig. 1. The material parameters used were obtained from Ishikawa<sup>11</sup> and are tabulated here for convenience (Table 1). Figure 1a shows magnetization as a function of time for multiple applied magnetic fields. As expected, for  $H = 0$  T, magnetization goes to zero at the Curie temperature ( $T_C = 1043$  K). We explored two cases of WMFT, where the quantum number is  $j = 1/2$  (solid lines) and  $j = 1$  (dashed lines). However, when subjected to an applied field, the alloy is still magnetized at temperatures over the Curie temperature. It is observed that the  $j = 1/2$  case yields a magnetization that is higher than the  $j = 1$  case. Figure 1b shows the percent difference between these two curves. It is shown that for small fields ( $H \lesssim 10$  T), there is a sharp increase in difference when  $T \sim T_C$ . This difference quickly plateaus to a maximum of approximately 10%. Further, it is shown that while the difference still increases monotonically for higher applied fields, there is a substantial decrease in the difference at higher temperatures.

To determine the magnetization, we need to numerically solve Eq. 8 to obtain  $\alpha$  at a given applied field and temperature. Since the solver requires an initial guess ( $\alpha_0$ ) for each condition, we assigned the previous temperature value to correspond to the current temperature initial guess:

$$\alpha_0^{(T+\Delta T, H=0)} \rightarrow \alpha^{(T, H=0)} \quad (27)$$

where  $\Delta T$  is the temperature discretization. Whenever this discretization is too large, a numerical instability is observed as  $T \rightarrow T_C$ , as shown in Fig. 2. For the  $\Delta T = 1$  K case, there is a large discontinuity very close to the Curie temperature. By decreasing the discretization to  $\Delta T = 0.95$  K, the discontinuity is mostly gone, and for  $\Delta T = 0.9$  K, no discontinuity is observed before the magnetization goes to

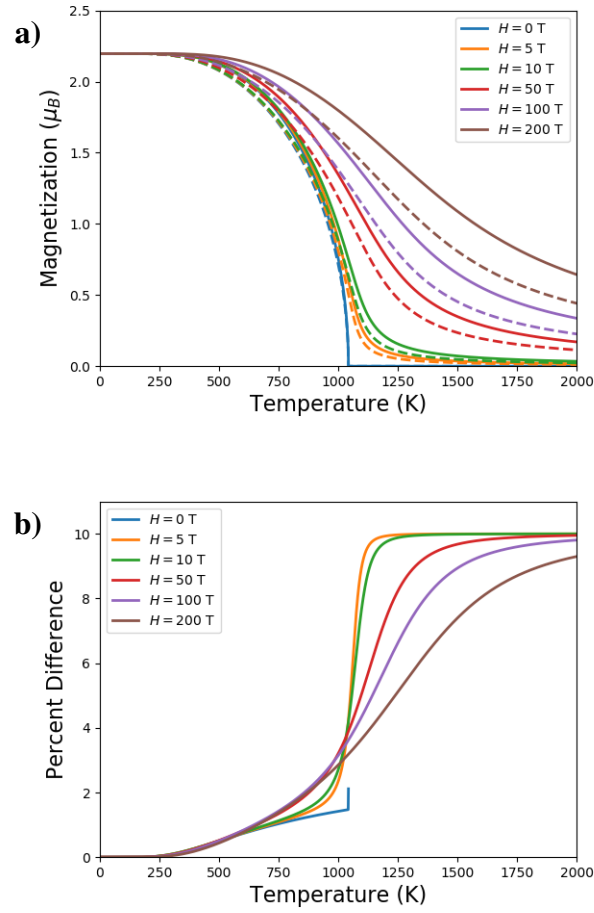


**Fig. 1** Fe magnetization as calculated by WMFT, showing a) curves for  $j = 0.5$  (solid) and  $j = 1$  (dashed) and b) the percent difference between the different  $j$  values. This shows that the error decreases as the applied field  $H$  increases.

**Table 1** Material parameters for WMFT, which describe the influence of alloying on the Curie temperature and magnetic moment in Fe (after Ishikawa<sup>11</sup>)

Alloying element	$dT_C/dx$ [ $^{\circ}C/at\%$ ]	$a$	$dm/dx$ [ $\mu_B$ ]	$b$
Co	12	1.15	1.11	0.5
Ni	-3.6	-0.34	1.30	0.59

$$a = 100/(dT_C/dx)/T_C^0 \quad b = (dm/dx)m^{Fe}$$

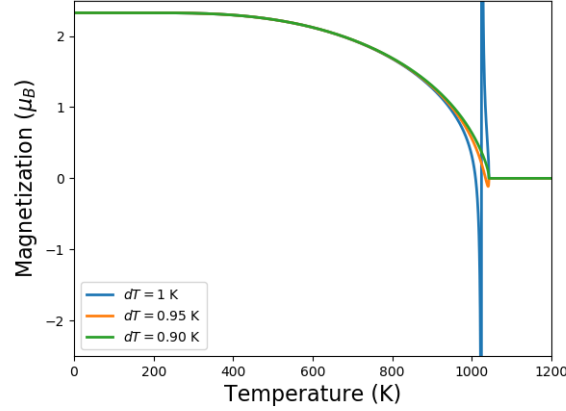


**Fig. 2** Instability observed for WMFT when calculating the magnetization for the Fe–10Ni alloy

zero. It should be noted that this instability was only observed when the alloying element causes the Curie temperature to decrease ( $T_C|_{x^M > 0} < T_C^{Fe}$ ). Furthermore, this anomaly was not observed when calculating magnetization under an applied field.

Figure 3 shows the magnetization as a function of alloying composition for the Fe-cobalt (FeCo) and Fe-nickel (FeNi) systems as predicted by WMFT. It is shown that the predicted values are often not realistic, especially for high alloy content (e.g.,  $M_0^{x^{Ni}=0.75} > 3\mu_B$  and  $T_C^{x^{Co}=0.75} \sim 1940$  K). Further, the shape of the magnetization curve is non-physical. This is likely due to the assumption that the Curie temperature and magnetic moment change linearly as a function of composition. While this might be a valid assumption for low alloying content, it is clearly not an accurate assumption otherwise, as discussed by Murdoch et al.<sup>5</sup>

### 3.2 KEoS Model

The EoS developed by Kuz'min based on Landau's theory was tested and compared against WMFT. This is shown for Fe in Fig. 4 for multiple applied magnetic fields, where the solid lines correspond to KEoS and the dashed lines correspond to WMFT. The material parameters used are shown in Table 2. Figure 4a shows that as the applied field increases the Kuz'min curves do not reach  $T = 0$  K. In fact, looking at Eq. 26 and setting the reduced magnetization to one ( $\sigma = 1 \rightarrow M = M_0$ ),

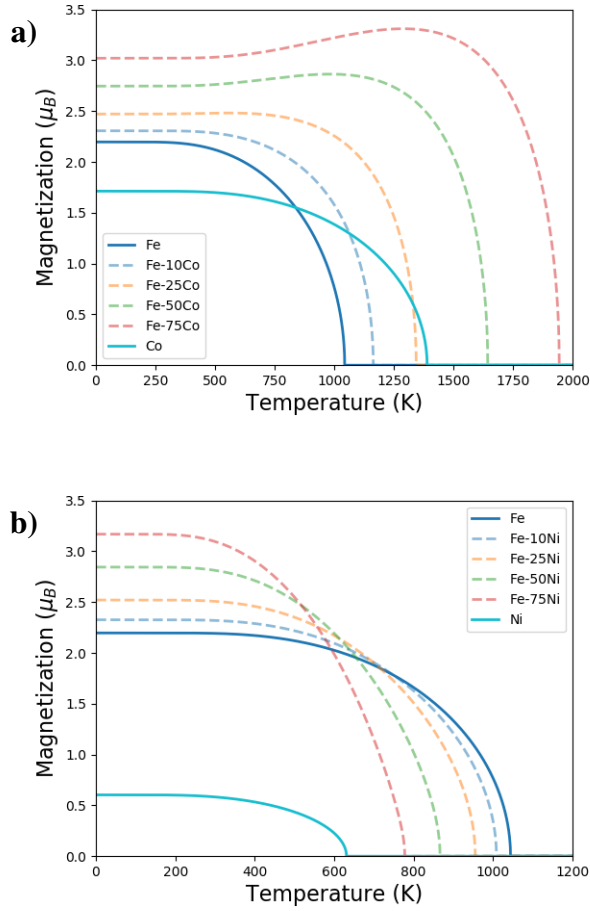


**Fig. 3** WMFT prediction of magnetization as a function of alloy composition for the a) FeCo and b) FeNi systems

we get

$$u = \frac{1}{2} \left[ 1 - \frac{H}{a_0} \right]. \quad (28)$$

Using this equation, we can determine the temperature at which KEoS predicts that the magnetization will be saturated, as shown in Fig. 4b. We can see that as the applied field increases, KEoS becomes less practical.

Figure 5 shows the KEoS prediction of the magnetization for the FeCo and FeNi systems at different compositions. Similar to the alloyed WMFT calculations, this model is unable to accurately predict realistic magnetization and Curie temperatures. This suggests that the adjustable KEoS parameters should be refit as the al-



**Table 2** Values of the parameters used for KEoS

Element	Fixed parameters		Adjustable parameters		
	$M_0$ (emu/g)	$T_C$ (K)	$p$	$\kappa$	$a_0$ (MOe)
Co	164	1390	0.25	0.43	3.7
Fe	222	1043	0.25	0.18	3.3
Gd	266	293	1.5	0.35	0.9
Ni	58	631	0.28	0.47	1.85

Note: Gd = gadolinium

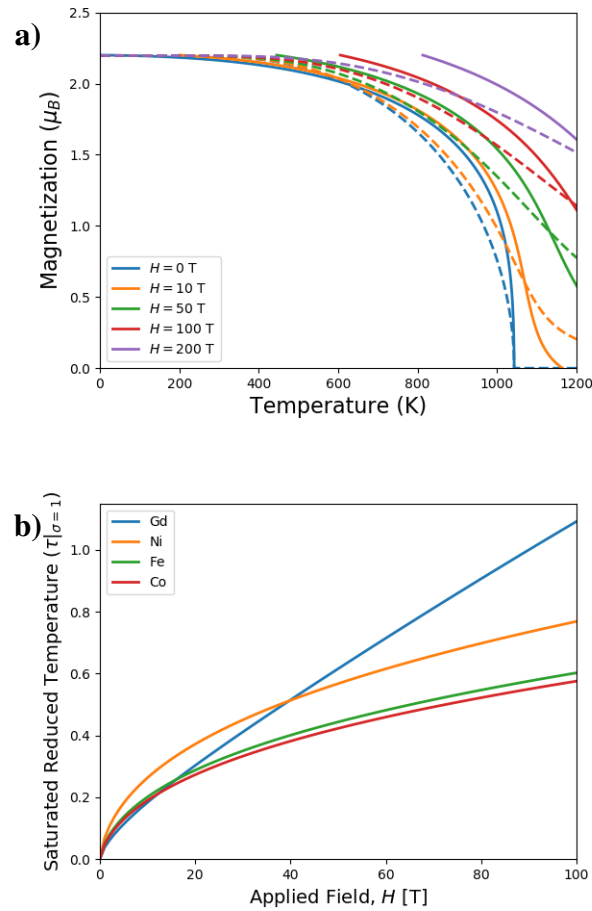


**Fig. 4** Performance of KEoS in predicting magnetization of Fe. a) Comparing the Kuz'min (solid) and WMFT (dashed) models, which show that there's a limit to Kuz'min as the applied field goes up. b) reduced temperature limit at the saturation magnetization ( $\tau|_{\sigma=1}$ ) as a function of applied field.

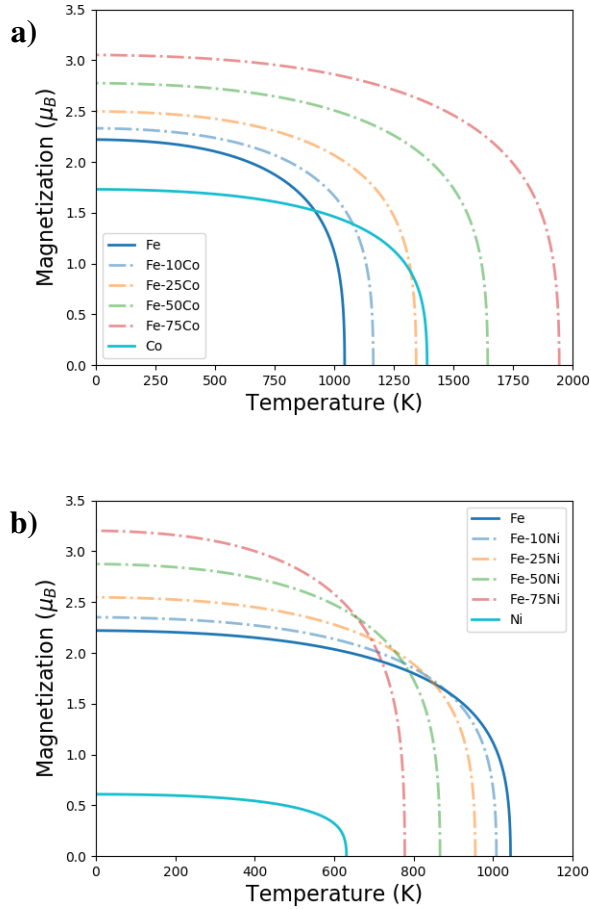


**Fig. 5** KEOs prediction of magnetization as a function of alloy composition for the a) FeCo and b) FeNi systems

loys undergo phase transformations. On the other hand, the KEOs model does not show the abnormal curve shape (bump) observed for the WMFT calculations.

### 3.3 Model Comparison

As a final analysis, the models were used to calculate the magnetization and compared against experimental values of pure Fe,<sup>12</sup> Ni,<sup>12</sup> and Co.<sup>13–15</sup> The resulting calculations are shown in Fig. 6. It is clear that KEOs better approximates the magnetization for pure alloys, followed by WMFT with a half-integer quantum number ( $j = 1/2$ ). Further, using  $j = 1/2$  with applied fields would require a discontinuity at  $T_C$  to make the ferro- and paramagnetic regions consistent with their respective

descriptions under WMFT as outlined by Murdoch et al.,<sup>5</sup> Guo,<sup>6</sup> and Bozorth.<sup>16</sup>

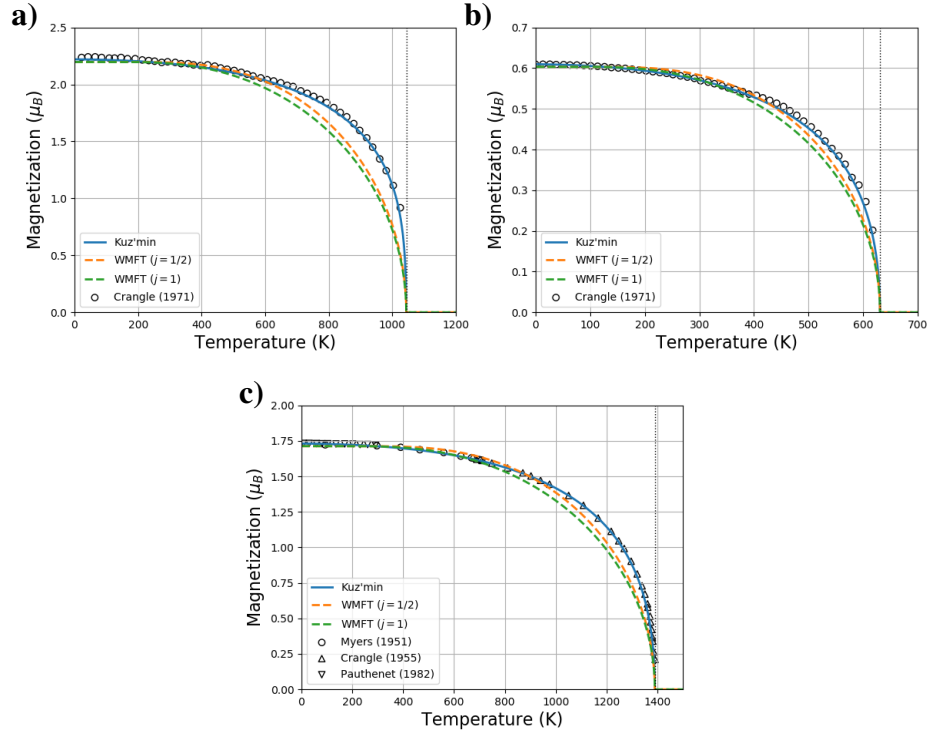


**Fig. 6** Comparison between WMFT and KEoS calculated magnetization for elemental a) Fe, b) Ni, and c) Co. It is clear that Kuz'min better approximates the experimental data.

## 4. Conclusions

The WMFT and KEoS models were used to calculate the magnetization of metals. A numerical instability was observed for WMFT as  $T \rightarrow T_C$ , which depends on the temperature discretization. Furthermore, it was shown that the assumption of a linear change in the Curie temperature and magnetic moment is invalid. KEoS was shown to perform best when no applied field is present, but encounters a low-temperature limit as the applied field increases. However, it performs better than the WMFT model at predicting the magnetization of pure metals at low applied fields.

## 5. References

---

1. Shimotomai M, Maruta K. Aligned two-phase structures in Fe–C alloys. *Scripta materialia*. 2000;42(5).
2. Zhang Y, Esling C, Calcagnotto M, Gong M, Zhao X, Zuo L. Shift of the eutectoid point in the Fe–C binary system by a high magnetic field. *Journal of Physics D: Applied Physics*. 2007;40(21):6501.
3. Zhou Z, Wu K. Molybdenum carbide precipitation in an Fe–C–Mo alloy under a high magnetic field. *Scripta Materialia*. 2009;61(7):670–673.
4. Hou T, Wu K, Liu W, Peet M, Hulme-Smith C, Guo L, Zhuang L. Magnetism and high magnetic-field-induced stability of alloy carbides in Fe-based materials. *Scientific reports*. 2018;8(1):1–10.
5. Murdoch H, Hernández-Rivera E, Giri A. Modeling magnetically influenced phase transformations in alloys. *Met Mat Trans A*. 2020 (under review).
6. Guo H, Enomoto M. Influence of magnetic fields on  $\alpha/\gamma$  equilibrium in Fe–C (–X) alloys. *Materials Transactions, JIM*. 2000;41(8):911–916.
7. Enomoto M, Guo H, Tazuke Y, Abe Y, Shimotomai M. Influence of magnetic field on the kinetics of proeutectoid ferrite transformation in iron alloys. *Metallurgical and Materials Transactions A*. 2001;32(3):445–453.
8. Landau L. On the theory of phase transitions. *Zh Eksp Teor Fiz*. 1937;7:19–32.
9. Kuz'min M. Landau-type parametrization of the equation of state of a ferromagnet. *Physical Review B*. 2008;77(18):184431.
10. Ginzburg V. *Zh Eksp Teor Fiz*. 1947;17:833.
11. Ishikawa Y. Handbook of magnetic substance. Chikazumi S, et al., editors. Tokyo: Asakura Shoten; 1975.
12. Crangle J, Goodman G. The magnetization of pure iron and nickel. *Proceedings of the Royal Society of London. A. Mathematical and Physical Sciences*. 1971;321(1547):477–491.

13. Myers H, Sucksmith W. The spontaneous magnetization of cobalt. Proceedings of the Royal Society of London. Series A. Mathematical and Physical Sciences. 1951;207(1091):427–446.
14. Crangle J. LIX The magnetic moments of cobalt-copper alloys. The London, Edinburgh, and Dublin Philosophical Magazine and Journal of Science. 1955;46(376):499–513.
15. Pauthenet R. Experimental verification of spin-wave theory in high fields. Journal of Applied Physics. 1982;53(11):8187–8192.
16. Bozorth RM. Ferromagnetism. Wiley–VCH; 1993.

**Appendix A. Weiss Mean Field Theory (WMFT) and Kuz'min's  
Equation of State (KEoS) Python Script**

---

```

1 '''
2 =====
3 : class : `magnetization` -- WMFT and Kuz'min EoS magnetization
4 =====
5
6 This module calculates the magnetization for a variety of alloys
7 as prescribed by the WMFT and the equation of state developed
8 by Kuz'min.
9
10 Developed by Efrain Hernandez-Rivera (2019--2020)
11 US Army Research Laboratory
12 --
13 THIS SOFTWARE IS MADE AVAILABLE ON AN "AS IS" BASIS
14 WITHOUT WARRANTIES OR CONDITIONS OF ANY KIND, NEITHER
15 EXPRESSED OR IMPLIED
16 '''
17
18 import numpy as np
19 from sympy import *
20 import matplotlib.pyplot as plt
21
22 #atomic masses
23 Me = {'Ni':58.6934, 'Co':58.933195, 'Fe': 55.845, 'Gd':64}
24
25 #constants
26 k = 1.38e-23 # J/K
27 N0 = 8.49e28 # #Fe/m3
28 muB = 9.274e-24 # J/T
29
30 Na = 6.02214076e23
31 fa = 4*pi*1e-7 # funky magnetic conversion
32
33 #from Guo and Enomoto, Mat Trans JIM 41.8 911-916 (2000)
34 # note: a=100/Tc0*dTc/dx, b=1/mFe*dm/dx
35 coefs={'V': {'dTdx':7.5, 'a':0.72, 'dmdx':-2.68,'b':-1.22},\
36         'Cr':{'dTdx':-1.5,'a':-0.14,'dmdx':-2.29,'b':-1.04},\
37         'Mn':{'dTdx':-15.,'a':-1.44,'dmdx':-2.11,'b':-0.96},\
38         'Co':{'dTdx': 12.,'a':1.15, 'dmdx':1.11, 'b':0.5},\
39         'Ni':{'dTdx':-3.6,'a':-0.34,'dmdx':1.3, 'b':0.59},\
40         'Mo':{'dTdx':0., 'a':0., 'dmdx':-2.11,'b':-0.96},\
41         'Si':{'dTdx':-3.5,'a':-0.34,'dmdx':-2.29,'b':-1.04},\
42         'labs':['dTc/dX', 'a', 'dm/dx', 'b']}

```

```

42 #from Kuz'min, PRB 7 184431 (2008)
43 # note: M0 (emu/g) Tc (K), p, kappa, a0 (MOe)
44 #      : 1 [emu] = 1.078283e20[uB]
45 #      : 1 [emu/g] * 1.078283e20 [uB/emu] * Ma [g/mol] / Na [mol/
      atom]
46 kuz ={'Gd':{'M0':266, 'Tc':293, 'p':1.50, 'k':0.35, 'a0':0.9},\
47       'Ni':{'M0':58, 'Tc':631, 'p':0.28, 'k':0.47, 'a0':1.85},\
48       'Fe':{'M0':222, 'Tc':1044, 'p':0.25, 'k':0.18, 'a0':3.33},\
49       'Co':{'M0':164, 'Tc':1390, 'p':0.25, 'k':0.43, 'a0':3.70}}
50
51 class magnetization(object):
52     '''
53     Class to calculate magnetization curves as a function of
54     temperature
55
56     Inputs:
57
58         a, b : Coeficents for calculation of the Curie
59         temperature and magnetic moment, respectively. Values for
60         several alloying elements (V, Cr, Mn, Co, Ni, Mo, Si) can be
61         called as follows:
62
63         >>> E = 'Ni'
64         >>> a, b = coefs[E]['a'], coefs[E]['b']
65
66         [Guo and Enomoto, Mat Trans JIM 41.8 911-916 (2000)]
67
68         Tc   : Curie temperature (K)
69
70         H    : Magnetic field intensity (T)
71
72         j    : Angular momentum quantum number, should be a
73         multiple of 1/2 (optional, default=1)
74
75         maxT : Maximum temperature (K) to which magnetization is
76         determined (optional, default=1100)
77
78         dT   : Discretization step for the temperature array (
79         optional, default=0.1)
80
81         m0   : Magnetic moment of pure iron (mu_B) (optional,
82         default=2.2)
83
84     '''

```



```

76
77 def __init__(self, a, b, Tc, H, j=1., maxT=1100, dT=0.1, m0=2.22):
78     self.a = a
79     self.b = b
80     self.j = j
81     self.m = muB*m0 # [Bohr magneton]
82     self.Tc = Tc # [K]
83     self.H = H # [T]
84     self.maxT = maxT # maximum T to analyze [K]
85     self.dT = dT # temperature discretization
86
87     self.alpha, self.T = symbols('alpha T')
88
89     self.Bj = (self.j+0.5)/self.j*coth(self.alpha*(self.j
90 +0.5)/self.j)\
91             - 0.5/self.j*coth(0.5*self.alpha/self.j)
92     self.dBj = diff(self.Bj, self.alpha)
93
94     self.alphaSol = []
95
96 def solveAlpha(self, a0=1000):
97     '''
98     Solve WMFT for pure system, obtaining alpha parameters.
99     Function will loop from 1 to Tm in 1 K increments.
100
101     Inputs:
102     a0 : Initial guess for alpha (optional, default
103 =1000)
104
105     Outputs:
106     alphaSol : Array of alpha values between 1 K and Tm
107     '''
108
109     j, m, alpha, T, Tc = self.j, self.m, self.alpha, self.T,
110 self.Tc
111     eq = (j+1)/3./j*T/Tc*alpha - (j+1)/3./j*m*self.H/Tc/k
112     dT = np.arange(1, int(self.maxT)+1, self.dT)
113
114     for t in dT:
115         self.alphaSol.append(nsolve((eq.subs(T,t) \
116 - self.Bj), (alpha), (a0)))
117         a0 = self.alphaSol[-1]

```

```

115     def calcMag(self,X,i=0):
116         '''
117             Calculate temperature dependent magnetization for given
118             alloying concentration
119
120             Inputs:
121                 X : Concentration of alloying element
122
123             Outputs:
124                 M : Array of magnetization values between 1 K and
125                 maxT
126         '''
127         a, b, j, alpha = self.a, self.b, self.j, self.alphaSol[i]
128         m = self.m#*(1+b*X)
129         Tc = self.Tc#*(1.+a*X)
130         T = Tc*(1+a*X)*float(i)/Tc
131
132         Bj = self.Bj.subs( self.alpha,alpha)
133         dBj = self.dBj.subs(self.alpha,alpha)
134
135         A = (k*T*a*alpha + (b-a)*m*self.H)/(k*T - 3.*k*self.Tc*j*
136         dBj/(j+1.))
137         M = fa*m*N0*(Bj + (dBj*A + Bj*b)*X)
138         return M
139
140     def landau(self,sig,m0=2.22,X=0.,p=0.25,k=0.18,a0=3.3):
141         '''
142             Calculate magnetization of pure Fe using Kuz'min
143             application of Landau
144             [Kuz'min, Phys Rev B 77, 184431 (2008)]
145
146             Inputs:
147                 sig      : Array for the reduced magnetization (M/M0
148                 )
149
150                 p, k, a0 : Fitting parameters for pure Fe as
151                 determined by Kuz'min (optional, default= 0.25, 0.18, 3.3)
152
153             Outputs:
154                 [T, m] : Array of temperature and magnetization
155                 values between 1 K and Tc

```

```

151
152     '''
153
154     H = self.H/1e2 #field given in T
155     u = 0.5*(k*sig**2. + (1.-k)*sig**4. - (H/(a0*(sig+1e-1))))
156     t = ((1 - 2*u + p*p*u*u)**0.5 - p*u)**(2/3.)
157
158     return np.array([t*self.Tc*(1+self.a*X), sig*m0*(1+self.b*
159 X)])
160 if __name__=='__main__':
161     E='Ni'; dT = 0.5; maxT = 2000
162     T = np.arange(1,maxT+1,dT); n = T.size
163     m0 = kuz[E]['M0']*1.078283e20*Me[E]/Na
164     Tc = kuz[E]['Tc']
165     wmft = magnetization(0,0,Tc,0,maxT=maxT, dT=dT, j=0.5, m0=m0)
166     wmft.solveAlpha()
167     M=np.array([wmft.calcMag(0,i=i) for i in range(n)])
168
169     data = wmft.landau(np.linspace(1e-5,1,100001),p=kuz[E]['p'],k=
170 kuz[E]['k'],a0=kuz[E]['a0'],m0=m0)
171
172     plt.plot(data[0],data[1],label=r"Kuz'min",lw=2)
173     plt.plot(T,M,'--',label=r'WMFT ($j=1/2$)',lw=2)
174
175     wmft = magnetization(0,0,Tc,0,maxT=maxT, dT=dT, j=1., m0=m0)
176     wmft.solveAlpha()
177     M=np.array([wmft.calcMag(0,i=i) for i in range(n)])
178
179     plt.plot(T,M,'--',label=r'WMFT ($j=1$)',lw=2)
180
181     plt.xlim(0,700)
182     plt.ylim(0,0.7)
183
184     plt.axvline(Tc,lw=1,ls=':',c='k')
185     plt.grid()
186
187     plt.xlabel('Temperature (K)',fontsize=16)
188     plt.ylabel(r'Magnetization ($\mu_B$)',fontsize=16)
189
190     plt.legend()
191     plt.show()

```

## List of Symbols, Abbreviations, and Acronyms

---

### TERMS:

Co	cobalt
Fe	iron
Ni	nickel
Gd	gadolinium
KEoS	Kuz'min's equation of state
WMFT	Weiss mean field theory

### MATHEMATICAL SYMBOLS:

$\mu_0$	permeability of vacuum
$\sigma$	reduced magnetization
$\tau$	reduced temperature
$B_j$	Brillouin function
$H$	applied magnetic field
$M$	magnetization
$M_0$	saturation magnetization
$N$	atomic density
$T$	temperature
$T_C$	Curie temperature
$j$	quantum number
$k_B$	Boltzmann constant
$m$	magnetic moment
$x$	alloying composition

1 DEFENSE TECHNICAL  
(PDF) INFORMATION CTR  
DTIC OCA

1 FCDD RLD DCI  
(PDF) TECH LIB

13 DIR CCDC ARL  
(PDF) FCDD RLD  
H MAUPIN  
M TSCHOPP  
FCDD RLW  
A RAWLETT  
FCDD RLW M  
E CHIN  
J LASCALA  
FCDD RLW MB  
E HERNANDEZ  
B LOVE  
FCDD RLW MD  
K CHO  
FCDD RLW ME  
M GUZIEWSKI  
S SILTON  
FCDD RLW MF  
K DOHERTY  
A GIRI  
H MURDOCH